Oahu Distributed PV Grid Stability Study

Part 1: System Frequency Response to Generator Contingency Events

Prepared for the

U.S. Department of Energy
Office of Electricity Delivery and Energy Reliability

Under Cooperative Agreement No. DE-EE0003507
Hawai‘i Energy Sustainability Program

Task 2: Energy Modeling and Scenario Analysis

Prepared by

GE Energy Consulting

Submitted by

Hawai‘i Natural Energy Institute
School of Ocean and Earth Science and Technology
University of Hawai‘i

March 2016

Acknowledgement: This material is based upon work supported by the United States Department of Energy under Cooperative Agreement Number DE-EE0003507.

HNEI
Hawai‘i Natural Energy Institute
School of Ocean and Earth Science and Technology
University of Hawai‘i at Mānoa

Oahu Distributed PV Grid Stability Study

Part 1: System Frequency Response to Generator Contingency Events

Prepared for: Hawaii Natural Energy Institute
Prepared by: GE Energy Consulting
Date: March 3, 2016

Foreword

In the fall of 2015, GE Energy Consulting and the Hawaii Natural Energy Institute began a technical assessment of the Oahu power grid, with a goal of utilizing power system models to understand and quantify the impact of increasing variable renewable energy technologies, specifically distributed photovoltaic (DPV) energy, on system stability, reliability, and economics. This report is the first phase of a multi-faceted project that will cover several topics of renewable integration. While this report is meant to be a stand-alone document and can be read independently of the other project phases, it should be viewed in a larger context. This report will not address all questions or topics related to grid stability and renewable integration, but will refer readers to additional scope that will be the subject of future analysis.

This report was prepared by General Electric International, Inc. ("GEII"); acting through its Energy Consulting group ("GE Energy Consulting") based in Schenectady, NY, and submitted to the Hawaii Natural Energy Institute ("HNEI"). Questions and any correspondence concerning this document should be referred to:

Technical Contact

Derek Stenclik

Manager, Power Systems Strategy

GE Energy Consulting

General Electric International, Inc.

One River Road

Building 53

Schenectady, New York 12345

Phone: 434-978-5052

Fax: (518) 385-5703

E-Mail: derek.stenclik@ge.com

Project Team

GE Energy Consulting

Derek Stenclik

Matthew Richwine

Richard Piwko

Hawaii Natural Energy Institute

John Cole

Richard Rocheleau

Kevin Davies

Technical Review Committee

Hawaii Public Utilities Commission (HPUC)

Hawaiian Electric Company (HECO)

Department of Business, Economic Development, and Tourism (DBEDT)

Division of Consumer Advocates

Brendan Kirby

Sebastian Nola

TABLE OF CONTENTS

LIST OF FIGURES

LIST OF TABLES

1 INTRODUCTION

1.1 Study Overview & Objectives

The Hawaiian electric power industry is at a critical nexus; renewable technologies such as wind and solar are a rapidly growing portion of the islands' overall energy mix, the Hawaii State Legislature recently passed the country's most progressive renewable energy policy (requiring 100% of electricity to be produced by renewable technologies by 2045), and the state's primary utility, the Hawaiian Electric Company (HECO), is currently involved in a merger and acquisition. As a result, Hawaii's power grids are transforming quickly. At the end of 2015, the Oahu grid had over 343 MW of distributed solar PV (DPV) systems,[1] leading the nation in distributed solar adoption and continuing to grow. At the same time, the Hawaii Public Utilities Commission (PUC) approved approximately 140 MW of additional utility-scale solar PV projects, which may come online before the end of 2017.

With considerable changes taking place on the system, robust engineering and economic planning studies are critical. There are several ongoing analyses and modeling efforts underway or recently completed addressing renewable integration plans and challenges. Most notably, HECO is performing additional analysis required for the Power Supply Improvement Plan,[2] which outlines the utility's long-term outlook with specific attention towards renewable integration efforts. Additional production cost and long-term planning analyses, including those performed by GE Energy Consulting and the Hawaii Natural Energy Institute (HNEI), have focused on the annual and hourly impact of renewables on system operations and economics.

While production cost and capacity expansion studies are a necessary part of system planning, they do not evaluate the dynamic performance of the grid during critical operating periods and contingency events. This second type of analysis, dynamic simulation, focuses on the grid's performance over the course of seconds, or fractions of seconds, during critical periods of operations. It is important to evaluate and understand the grid's dynamic performance because as wind and solar integration increases, there is a potential for the grid's dynamic performance to erode. If this occurs, the grid will be more vulnerable to critical disturbances and may increase the likelihood of an island-wide grid blackout. This is because wind and solar generators are fundamentally different from conventional thermal synchronous machines. As wind and solar begin to displace conventional thermal generators, the system may lose important ancillary services to maintain the grid's dynamic performance. While wind and solar can provide many of these critical services it will require a shift in grid operations and better understanding of their impacts on frequency response.

[1] Hawaiian Electric Company, "Quarterly Installed PV Data, 4th Quarter 2015," https://www.hawaiianelectric.com/clean-energy-hawaii/going-solar/more-solar-information

[2] Hawaiian Electric Company, "Power Supply Improvement Plan," HPUC Docket 2014-0183, Commission Order No. 33320, February 16, 2016.

In addition, much of the dynamics work that was done in the past focused on a select few number of operating points, often evaluating only the very extremes of system operation. While it is necessary to ensure grid stability and reliability at all times, it is important to understand the regularity and magnitude of critical operating periods. This understanding will ensure that mitigations to prevent or avoid grid stability challenges will be properly evaluated. For example, low-probability events may be best addressed using changes to operating practices or even under-frequency load shedding because the probability of occurrence is low, whereas high-probability events may be better addressed with new technologies and capital investments.

To address the need for additional analysis, this study was performed to evaluate the grid stability and dynamic performance of the Oahu power grid with increasing levels of renewable penetration, with a particular emphasis on the growth of distributed photovoltaic (DPV) solar resources. DPV was the primary focus of this study because it is the fastest growing renewable energy resource in Hawaii, is currently uncontrolled by the grid operator, and currently does not provide frequency response services to the grid. This study also focuses on the system's frequency response to a large loss of generation event (N-1 generator contingency) only. Other aspects of grid stability, including loss of load events and grid strength, will be evaluated in later stages of analysis, documented in follow-on reports.

In addition, this study attempts to provide a better link between the dynamic grid simulations and the production cost analysis. To do this, the study created a composite frequency stability metric that was used to screen for potentially challenging hours from the production cost simulations and long-term planning analyses, without having to perform time consuming dynamic simulations for each operating point throughout the year. This was achieved by a careful examination of key variables associated with grid frequency response, and a close calibration of this composite metric to the outputs of dynamic simulations.

The remainder of this report discusses the methodology of the analysis, analytical results of modeling simulations, potential mitigation strategies, and key observations for Oahu's frequency response with increasing DPV.

1.2 Overview of Frequency Response

A common characteristic of all power grids is the requirement that generation (supply) and system load must be balanced at all times. This balance is measured by system frequency. North American and Hawaiian power grids operate at a nominal frequency of 60 Hz. If generation is higher than load, frequency rises above 60 Hz; if generation is lower than load, frequency declines below 60 Hz. Given that the load on the system is constantly changing throughout the day, generation resources must constantly adjust their output to regulate grid frequency back to 60 Hz. PV generation, which constantly changes its output as a function of irradiance from the sun, further complicates this situation and puts more duty on generators that can regulate frequency.

While minor fluctuations in grid frequency are normal and expected, large deviations are a risk to grid stability. Loads and/or generators may begin to trip offline and grid collapse (black-out) becomes a possibility.

It is particularly important that frequency be properly regulated in response to critical emergency events. If a conventional generator trips offline, the power system loses generation immediately and system frequency declines rapidly. These changes occur within a few seconds and corrective actions must be taken within those few seconds to restore balance and avoid a grid collapse. While large generator trips are not common, the grid operator must manage the grid to prepare for such events. Generally speaking, when this occurs the remaining online generating units quickly increase output to restore balance. This is controlled by the generator's governors, which automatically detect a grid disturbance and change output accordingly. As other generators increase their output, the decline in frequency slows and ultimately the frequency begins increasing towards 60 Hz. This inflection point is referred to as the frequency nadir and is the lowest point in system frequency following a contingency event. Over the course of about 30 seconds, the system will stabilize at a new quasi-equilibrium settling point. The change in power output from controlled resources (mostly generators) is called frequency response. Figure 1 provides an illustrative example of system frequency during a large generator trip event with the following points demarcated:

- **A:** Initial condition, system is stable at nominal frequency of 60 Hz, generator trip event occurs at time = 10 seconds.
- **A→C:** Frequency declines rapidly because system load exceeds generation.
- **C:** System frequency eventually stops declining at the nadir (C) when other generation resources increase their output or system load is reduced (shed) to restore balance between load and generation.
- **C→B:** System frequency "backswing" towards 60 Hz as other generators or loads respond to the contingency event.
- **B:** System recovers to a new stable equilibrium. The new equilibrium at 30 seconds may not be equal to the initial condition (60Hz). The final restoration to 60 Hz normally takes a little longer, through the operation of automatic generation control (AGC) or by re-dispatch of thermal units.

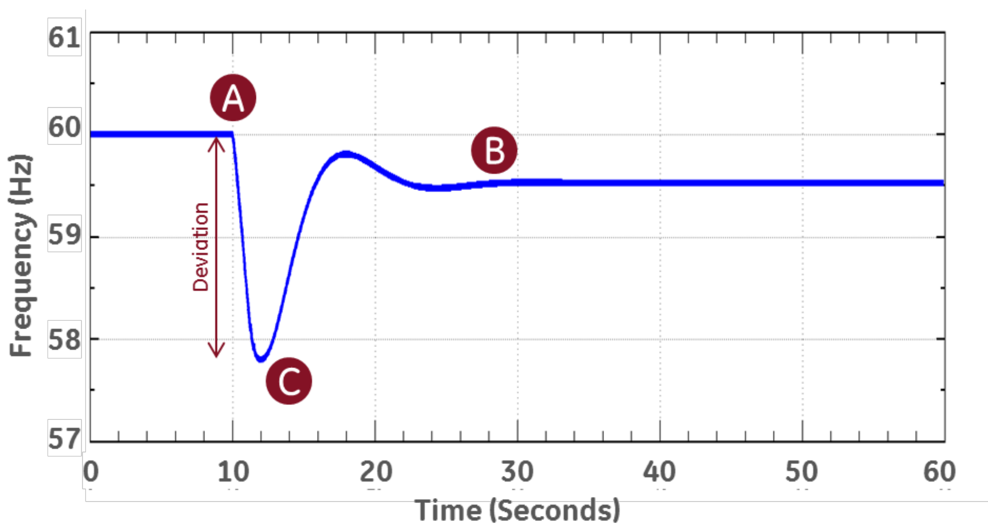

Figure 1: Illustrative Example of System Frequency Response to a Generation Trip

As is the case with many island power grids, the Oahu grid is unique relative to large interconnected power systems. A relatively small fluctuation in either generation or load can lead to large, and potentially unstable, deviations in system frequency for several reasons;

1. **Large Single Contingency:** Oahu's largest generating unit, the AES coal plant, is large relative to overall system load and to other thermal generating units on the system. With 200 MW of gross capacity the unit can, at times, account for up to 30% of the grid's total load, and up to 50% of the grid's net load (load minus wind and solar output). AES is also 34% larger than the next largest thermal unit on the system. As a result, a generator trip event of AES will lead to a substantial loss of generation and frequency excursion. It also defines the hourly contingency reserve requirement maintained by the system operator.
2. **Low number of synchronous generators**: Relative to large interconnected grids, Oahu has a low number of other synchronous generators online and available to provide primary frequency response. In addition, some generators like H-Power do not have governors enabled and therefore do not provide primary frequency response.
3. **No interconnections to neighboring systems:** The Oahu power grid is an isolated system. Large interconnected grids in North America can lean on neighbors during contingency events for support. Hawaii does not have this luxury and must provide all frequency response locally.
4. **High Level of Distributed PV Penetration:** The Oahu grid has very high penetration of DPV. While many of the DPV inverters have been upgraded to include frequency ride-through capability, there are still some legacy PV systems online (about 70 MW) that do not have this feature available. As a result, if system frequency declines below 59.3 Hz, the legacy PV will trip offline as well, increasing the magnitude of the original contingency event and causing the system frequency to decline even further.

As a result, the Oahu grid operators rely on a combination of generator governor response and under frequency load shedding (UFLS) during contingency events. The current UFLS scheme has several set points to shed load in an effort to halt the decline in system frequency. As frequency declines, distribution feeders will be disconnected from the grid to quickly reduce system load and balance supply and demand. UFLS is very effective in arresting system frequency decline, making it a powerful tool for maintaining overall grid stability. However, it interrupts customers' electric service without notice and should therefore only be used rarely, as a measure of last resort. With the increase in penetration of DPV on load feeders, the net load available to respond during UFLS events is reduced when DPV generation is high, thereby reducing the effectiveness of UFLS to protect grid stability.

Thus, it is critical to understand the impact of increasing DPV on Oahu's system frequency response and to better understand alternative tools and mitigations available to the utility to enhance grid stability. These may include frequency response provision from variable renewable energy sources (both utility-scale and distributed), energy storage, electric vehicles, and demand response.

1.3 Scope & Limitations

While this study significantly expands the technical analysis into areas not examined in previous studies, it is not exhaustive in covering all possible risks and mitigations for grid frequency stability. In particular the following points highlight the scope and potential limitations of the study:

- This study does not replace existing analysis conducted by the utility, state regulator or other stakeholders in Hawaii. Instead it is intended to supplement those studies with additional technical analysis and findings.
- This study evaluated generator contingencies only. It did not evaluate other important aspects of grid stability such as load contingency events or short-circuit ratios. This report represents Part 1 of a broader ongoing project that will evaluate additional aspects of grid stability and renewable integration.
- This study evaluated grid operations on Oahu only and did not perform simulations on other islands. Oahu was the focus of this study because it is the primary load center of Hawaii (over 70% of the state's electricity demand) and thus will require substantial renewable capacity additions in order to comply with the state's RPS targets.
- This study evaluated variable renewable capacity up to 974 MW (124 MW of wind, 150 MW of utility-scale solar and 700 MW of DPV). While this represents a substantial increase to today's installed renewables, findings should not be extrapolated beyond this level of renewable integration. Grid stability and operational challenges are non-linear and will require additional analyses to better understand higher penetration levels.
- This study analyzed system operation at the bulk-transmission grid level. It did not analyze individual distribution feeders or the circuit loading issues that may result from high levels of distribution-connected rooftop PV systems.
- The study is based on fundamental frequency, positive sequence analytical tools and models. While these are the basic and appropriate tools for analysis of frequency response, not all aspects of the dynamic performance and stability of inverter-based resources, including PV generation, are captured by them. Other types of high frequency and high bandwidth instabilities could conceivably present a risk.

2 METHODOLOGY

2.1 Analytical Process & Modeling Tools

To analyze the impact of increasing DPV penetration on system frequency response, a variety of models and statistical techniques were employed in this analysis to simulate both system operations and dynamic grid stability. While these models are not measuring real system conditions, they have been routinely benchmarked and validated against historical operations and are consistent with engineering practices utilized by HECO and other industry stakeholders. The methodology employed in this analysis included four steps as illustrated in Figure 2.

Figure 2: Analytical Process

Step 1 - Production Cost Simulations (GE MAPS): The first step in the analysis was to conduct detailed hourly production cost simulations. The GE-MAPS production cost model simulates the power system operation on an hourly, chronological basis over the course of the year. The model simulates the system operator's unit commitment (on or offline) and dispatch (MW output) decisions necessary to supply the electricity load in a least cost manner, while appropriately reflecting transmission flows across the grid and simultaneously preparing the system for unexpected contingency events and variability. The chronological modeling is crucial to understanding renewable integration because it simulates chronological changes to electrical load and the underlying variability and forecast uncertainty associated with wind and solar resources.

This modeling was performed for two scenarios, along with intermediate steps, (outlined in Section 2.2) with increasing levels of DPV penetration. This step is an essential part of the analysis because as solar penetration increases, the model provides accurate changes in unit commitment, dispatch, spinning reserves and potential curtailment. The 8,760 hourly results from the production cost modeling are provided in Section 3.1 and the outputs were passed to Step 2 for further analysis.

Step 2 – Selecting System Dispatch Conditions for Dynamic Simulations: The second step in the analysis included a detailed review of the production cost simulations. This process selected system dispatch conditions that were passed from the production cost results to the dynamic frequency response simulations. To do this, four key variables were analyzed for each hour of simulation: size of the largest generator contingency, the amount of committed capacity with governor response enabled, the amount of spinning up-reserve provided by conventional thermal generators, and the amount of legacy DPV (without frequency ride through) generation. These four variables were then translated to a single numerical metric quantified for each hour and dispatch condition. This was performed across the scenarios analyzed, with increasing DPV penetration. Several representative hours and dispatch conditions (including load and unit dispatch) were then selected to be analyzed in greater detail in Step 3.

Step 3 – Dynamic Frequency Response Simulations (GE PSLF): Each of the hours selected in Step 2 were evaluated in greater detail through dynamic frequency response simulations using the GE PSLF model. Using the dispatch conditions provided by Step 2, including system load and unit generation, a loss of generation contingency event was simulated. To do this, the GE PSLF model simulated a trip of the largest online generator in each hour selected and measured the system response over the course of 60 seconds. Key metrics evaluated in this part of the analysis included frequency nadir (Hz), frequency deviation (difference between the steady state frequency and the nadir, Hz), UFLS (MW), and the change in power output from online generators (MW).

Step 4 – Estimating Frequency Response for all Dispatch Conditions: In the final step of the analysis, the results calculated in Step 3 were statistically evaluated to examine the relationship between the calculated metric and the system's frequency nadir. A quadratic regression was then estimated using frequency nadir as the dependent variable and the metric as the independent variable. The resulting equation was then used to estimate the frequency deviation and UFLS for each hour and dispatch condition of the year, across both Scenarios. This allows for a more complete picture of system risk, and the frequency of different risk levels, over the course of the year and a comparison with increasing DPV scenarios.

2.2 Scenario Overview

To evaluate the impact of DPV on grid stability, two scenarios were evaluated. Scenario 1 included 400 MW of installed DPV capacity and Scenario 2 had 700 MW of DPV installed. Note that intermediate scenarios were evaluated with incremental 100 MW DPV capacity additions, but only the scenarios with the lowest and highest installed DPV are discussed in this report. Scenario 1 represents the likely installed DPV capacity online by 2017, assuming a continuation of recent trends. Scenario 2 was analyzed to show the impact of increased DPV penetration and was identified as a system hosting capacity limit in a recent PUC docket filing.[3] The hourly chronological solar output profiles were scaled linearly between the two scenarios, and the spinning reserve requirements were adjusted accordingly (see section 2.3 for more information). All other inputs and assumptions were held constant across the scenarios, isolating any changes due to increased DPV penetration.

Figure 3 provides an overview of the installed renewable capacity and available energy (prior to potential curtailment) for each of the scenarios evaluated. In the absence of curtailment, annual wind and solar energy penetration would be between 16% in Scenario 1 to 22% in Scenario 2. Note that while production cost simulations and hourly screening were performed on all four scenarios, only Scenario 1 and Scenario 2 were evaluated in the dynamic simulations to provide a bookend analysis and to limit the number of dynamic

[3] Hawaiian Electric Company, "System Level Hosting Capacity," HPUC Docket 2014-0192, Commission Order No. 33258, December 11, 2015.

simulations required. In addition, the 700 MW of DPV selected in Scenario 2 is not intended to show a maximum amount of DPV on the Oahu grid, but rather to reflect potential near-term growth.

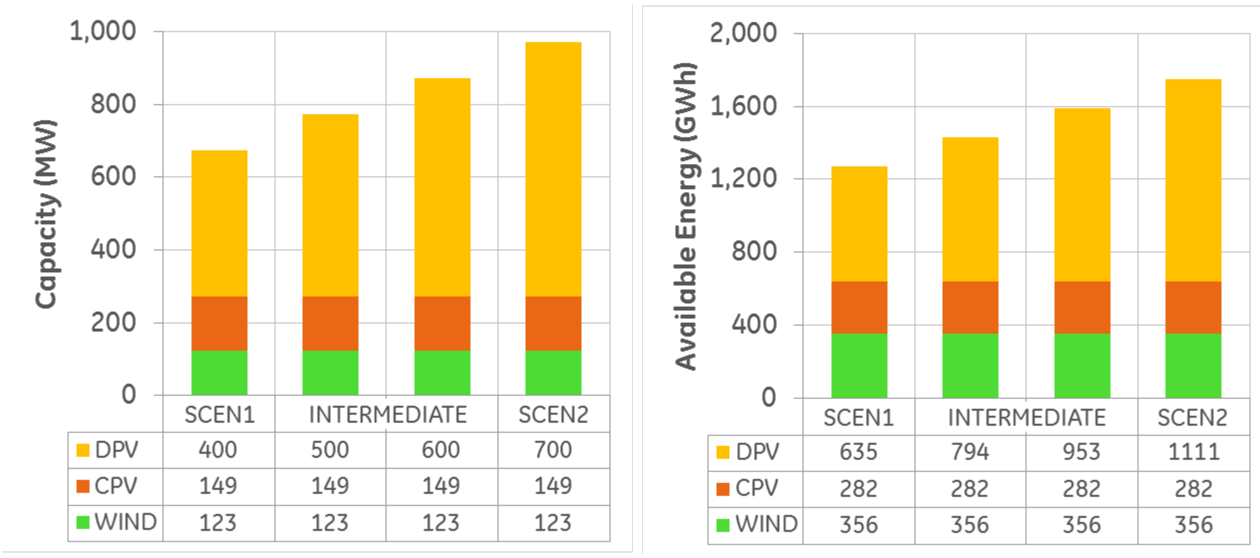

	SCEN1	INTERMEDIATE		SCEN2
DPV	400	500	600	700
CPV	149	149	149	149
WIND	123	123	123	123

	SCEN1	INTERMEDIATE		SCEN2
DPV	635	794	953	1111
CPV	282	282	282	282
WIND	356	356	356	356

Figure 3: Installed Wind & Solar Capacity & Available Energy by Scenario

2.3 Inputs & Assumptions

The inputs and assumptions used throughout the modeling efforts were developed in close collaboration with other modeling efforts in Hawaii, including previous studies conducted by GE Energy Consulting and the HECO Power Supply Improvement Plans. The study did not evaluate current grid configuration, but rather assumed a near-term grid configuration likely in the year 2017. GE Energy Consulting coordinated with HECO to ensure that all inputs and assumptions were current and utilizing the best available data. The following section provides an overview of high-level assumptions, with a more detailed overview of specific inputs and assumptions available upon request.

The GE MAPS production cost simulations included a detailed, nodal representation of the Oahu system, including:

- Distributed PV: 400 MW in Scenario 1, increasing to 700 MW in Scenario 2
- Utility-scale PV: 11 MW of existing solar plus approximately 140 MW of Waiver PV projects with PUC approval.
- Utility-scale Wind: Existing 99 MW of wind (Kahuku (30) and Kawailoa (69) wind plants), plus the proposed 24 MW Na Pua Makina wind plant.
- Wind and Solar Profiles: Hourly simulated production profiles for the year 2008, created for the Hawaii Solar Integration Study.
- Thermal generators: Current operating plants as of January 1, 2016 without any new installations or retirements (AES, Kahe 1-6, Kalaeloa CC, Waiau 2-10, CIP CT, Airport Biodiesel, and H-Power). Each generator was modeled with a high degree of fidelity, including maximum and minimum stable operating capacities (MW), incremental

heat rate curves (btu/KWh), variable operations & maintenance costs ($/MWh), and cycling constraints.

- Spinning Reserves: 180 MW of contingency reserves plus regulation reserves required for wind and solar variability.
- Thermal Unit Flexibility: Lower minimum stable operating levels (P-Min) on Kahe 1-4, and Waiau 7-8 consistent with the PSIP. Unit cycling (removed must-run constraints) allowed on Kahe 1-4.
- Load: Annual energy of 7,959 GWh and a peak demand of 1,223 MW.
- Fuel Price: $60/bbl of oil, adjusted to include refining delivery charges for a 70/30 LSFO-Diesel fuel blend for each unit.

Transmission System

The underlying powerflow model utilized during the production cost and dynamics simulations was provided by HECO in PSS/E format as their 2015 load flow case. The model included the Oahu network topology and major equipment ratings like transformer ratings. The network captures the lines and buses at the 46kV level and above, with lines and buses at lower voltages included for generation plants. A representation of the overall model is shown in Figure 4.

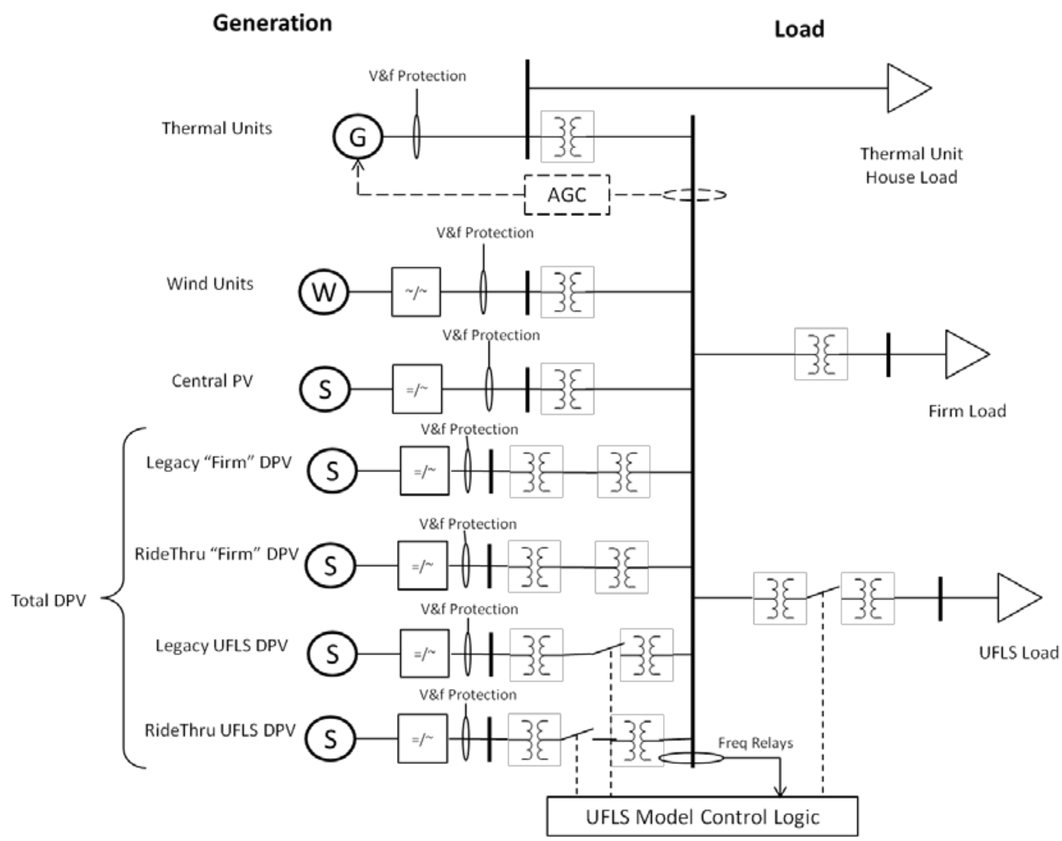

Figure 4: Overview of the Oahu Dynamic Simulation Model

Thermal Generation

For each thermal generation unit, a dynamic model that included the generator, exciter, and governor was used, based on inputs from HECO in their 2015 PSS/E Dynamics Record File (DYR). Frequency protection was modeled for the following thermal generators: Kalaeloa CC, Kahe 5-6, Waiau 7-8 with the assumed trip settings of +/-3Hz @ 2.0 seconds.

Wind Generation

Each wind turbine plant was modeled as an aggregate plant model, with the exception of the Na Pua Makina wind farm in which each turbine was modeled individually in the original load flow received. The dynamic models included the generator, converter, and turbine where the models and parameters are assumed to be values typical of utility-scale wind turbines with low-voltage ride-through features enabled and frequency ride-through capability of +1.5Hz / -3Hz @ 6.1 seconds; +3Hz/-3.5Hz @ 0.1 seconds.

Central PV Generation

Each central PV plant was modeled as an aggregate plant model with dynamic models that are assumed to be typical of utility-scale PV plants with low-voltage ride-through features enabled and frequency ride-through capability of +1.5Hz / -3Hz @ 6.1 seconds; +3Hz/-3.5Hz @ 0.1 seconds.

"Legacy" Distributed PV Generation

The distributed PV generation was modeled as 31 aggregate PV plants interspersed throughout the Oahu model. Each of the DPV models connects to a 480V bus, where an aggregate transformer with an impedance assumed to be typical of two transformers in series connect the 480V PV bus to the 46kV transmission system bus. A dynamic model of each DPV generator was used where the settings are typical of distributed PV systems.

The frequency ride-through settings were provided in the HECO model, and vary based on the classification of the DPV.

- "Legacy" DPV frequency trip settings: 59.3Hz @ 0.157 seconds; 60.5Hz @ 0.157 seconds
- "Ride-through" DPV frequency trip settings: 57.0Hz @ 0.157 seconds; 63.0Hz @ 0.157 seconds

Voltage relay settings were not implemented in the model.

The total DPV generation from MAPS was proportionally allocated among the 31 aggregate DPV models based on their original rating in the load flow, where the DPV was represented as a negative load. A "DPV fraction" was calculated by dividing the total DPV dispatched in the hour by the total DPV installed in the scenario. It was assumed that there is 70 MW of legacy DPV capacity. The "Legacy DPV" dispatched was assumed to be the resulting MW from multiplying the "DPV fraction" value by 70 MW legacy capacity.

It was assumed that 30% of the DPV capacity is installed behind one of the UFLS breakers, which assumes that the location of future DPV installations follows historical trends. It was further assumed that 30% of the DPV capacity that is installed behind one of the UFLS breakers is a legacy DPV unit. Because the legacy DPV will have tripped before the first UFLS block, this DPV is subtracted from the total DPV capacity in the UFLS scheme to result in a value for non-legacy DPV behind a UFLS breaker. This non-legacy DPV in the UFLS scheme is proportionally allocated among the 5 UFLS blocks and 2 kicker blocks according to UFLS data provided by HECO. Refer to Figure 4 for an illustrative representation of the four types of DPV.

Load

Static loads, with constant impedance, current, and power (ZIP), were used for all system loads, which are aggregated and connect at the 46kV level. The modeled loads are frequency-dependent, which is a conservative assumption for a generation trip analysis because any frequency-dependence to the load in reality will only increase the stability of the system in the event of a generation trip event. The total system load was split proportionally among 38 load buses according to their dispatch in the original load flow provided by HECO.

House loads, provided in Table 1, at several of the generation plants were modeled explicitly. During a generator trip event, it is assumed the house loads at the plant remain on at their pre-trip power level, which is a conservative assumption.

Table 1: Summary of Generator Plant Loads

Generator	House Load (MW)
Kahe 1,2,3	2.2
Kahe 4	3.4
Kahe 5,6	6.2
Waiau 7,8	3.6
Kalaeloa 1,2	2.0
AES	20.0

Under-Frequency Load Shedding (UFLS)

To complete the dynamic model, this information was augmented with details on the UFLS system and estimates of DPV affected by the UFLS system from HECO. This information was used to create logic to control the connection and disconnection of DPV and load to simulate the response of the UFLS scheme, in which system frequency is monitored and a selectable amount of load is tripped for a specified system frequency threshold and delay time. In addition, a selectable amount of DPV is tripped simultaneously with load, representing the DPV that is lost on feeders tripped by UFLS.

The load associated with each block of load shedding is determined by calculating the total load participating in the UFLS scheme for a given hour. This participating load is then proportionally allocated among the 5 load shedding blocks and two kicker blocks based on UFLS data provided by HECO in the same proportions used to allocate the DPV that falls behind the UFLS relays.

3 ANALYTICAL RESULTS

3.1 Production Cost Simulations

The hourly production cost simulations were performed for a chronological, 8,670 hour dispatch of the Oahu power system. This analysis takes into account the commitment and dispatch of both conventional thermal generators and wind and solar generators to serve the system load in a least cost manner. Included in the optimization are constraints on system operations including transmission constraints, fixed operating schedules of some baseload units (must-run status), spinning reserve provision for contingency events and wind and solar variability, minimum run times and down times, and generator outages.

The result of this analysis provides a chronological commitment and dispatch profile for the thermal units, delivered and curtailed wind and solar generation, total fuel consumption and production cost (fuel costs, variable operations and maintenance costs, and startup costs). The hourly simulation results were then screened for challenging hours of operation, and investigated in further detail for grid stability.

Figure 5 provides a visualization of a week of chronological system dispatch (Monday – Sunday) from the GE MAPS model output. The figure provides and illustrative example of how unit commitment and dispatch takes place over the course of a week. The upper envelope of the curve represents the total system load, while each colored band represents the output of a unit (or group of units). Thermal generating units are ranked, from the bottom up, based on their variable costs of generation and/or fixed operating schedules and must-run rules. Wind and solar generating units are shown on top. With the increased solar PV on the system, the overall change to the net load (total system load minus wind and solar power) is pronounced. During mid-day hours the baseload thermal generating units are backed down to near minimum loading levels. In addition, it can be observed that peaking units and some cycling units (Waiau 3-6) are utilized exclusively during the morning or evening hours during load ramps, or when the solar availability is lower (cloudy day). AES and H-Power, the most economic units on the system adjust output rarely.

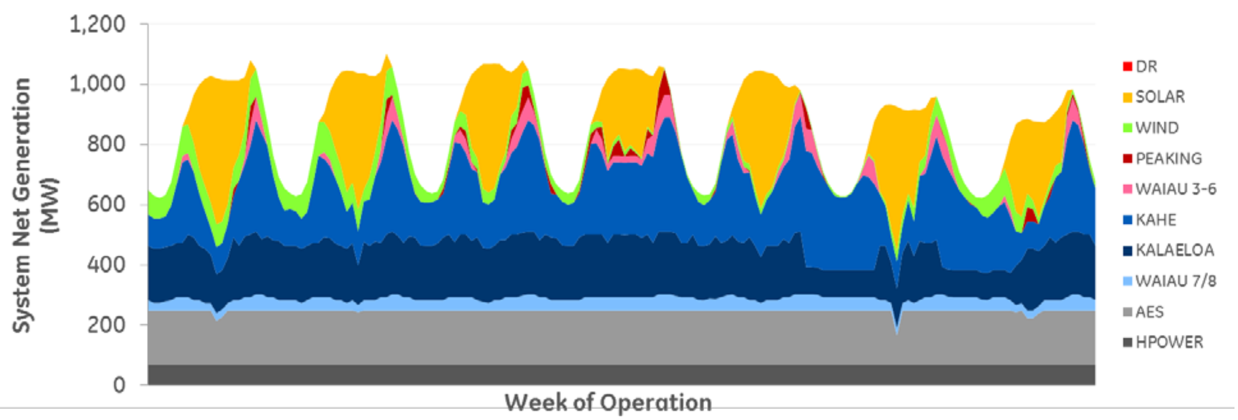

Figure 5: Weekly Chronological System Dispatch: Week 15, Scenario 1

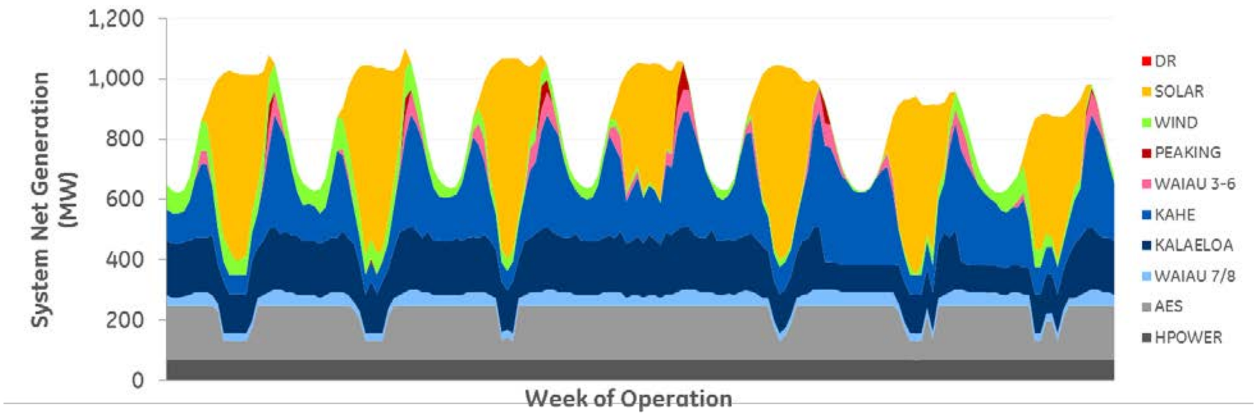

Figure 6: Weekly Chronological System Dispatch: Week 15, Scenario 2

The same week of operation is also shown in Figure 6, this time for Scenario 2, including an additional 300 MW of DPV capacity on the system. This allows for a direct comparison of the commitment and dispatch profiles across the two scenarios, isolating the impact of increased solar generation. Relative to Scenario 1, shown in Figure 5, the daily solar profiles are more pronounced, and the thermal unit cycling is increased. The thermal baseload units, shown in blue, decrease output substantially during the day-time hours, and often exhibit a flat "plateaued" operating profile. This represents times when the units are dispatched at minimum loading levels and cannot be turned down lower. If and when all units are dispatched at minimum load, the only remaining operating decision is to curtail wind or solar. In Scenario 2, even turn-down of AES becomes a regular operating procedure.

The production cost simulation, illustrated for one week in Figure 5 and Figure 6, is continued for the duration of the year. This allows for a complete screening of unit level commitment and dispatch for each hour of the year. The annual, aggregated results of this exercise are provided in Table 2 for both scenarios. From this table, several observations from a dynamic stability perspective can be made, highlighting the changes between the two scenarios as more distributed solar is brought online.

- H-Power, AES, Kahe 5&6, Waiau 7&8, and Kalaeloa CC-1 remain in fixed operating schedules based on current PPA structures, cogen requirements, lack of unit flexibility, or system voltage concerns. The annual hours online and annual starts do not change between the two scenarios. However, the units are turned down more often and have a lower annual generation and capacity factor with increased DPV generation.
- Kahe 1-4, Kalaeloa CC-2 and 3, Waiau 3-6 have a lower annual generation and capacity factor with increased DPV, and the number of cycles (on/off) increase. This indicates more hours of the year with decreased thermal unit commitment.
- Peaking utilization (Waiau 9-10, CIP-CT, and Airport diesel) experience a decrease in annual generation, but are required to cycle more.
- Wind and CPV plants exhibit slightly decreased generation due to increased curtailment as additional DPV is brought online.

Table 2: Annual Unit Utilization, Scenarios 1 and 2

Unit Name	Unit Type	Capacity (MW)	Scenario 1 Generation (GWh)	Scenario 1 Capacity Factor	Scenario 1 Hours Online	Scenario 1 Annual Starts	Scenario 2 Generation (GWh)	Scenario 2 Capacity Factor	Scenario 2 Hours Online	Scenario 2 Annual Starts
H-Power	ST-Waste	68.5	539.6	90%	8592	1	539.5	90%	8592	1
AES	ST-Coal	180.0	1422.4	90%	8064	1	1358.4	86%	8064	1
Kahe 1	ST-Oil	82.2	201.7	28%	4779	198	173.1	24%	4294	287
Kahe 2	ST-Oil	82.2	297.9	41%	6137	195	259.9	36%	5681	284
Kahe 3	ST-Oil	86.2	389.7	52%	7273	38	350.2	46%	7123	73
Kahe 4	ST-Oil	85.3	374.9	50%	6670	107	329.6	44%	6420	161
Kahe 5	ST-Oil	134.6	606.5	51%	5736	2	536.0	45%	5736	2
Kahe 6	ST-Oil	133.8	453.3	39%	6408	2	418.0	36%	6408	2
Waiau 7	ST-Oil	83.3	311.4	43%	7248	2	287.9	39%	7248	2
Waiau 8	ST-Oil	86.2	225.0	30%	6744	2	213.5	28%	6744	2
Kal-CC 1	CC-Oil	90.0	698.7	89%	7929	52	677.2	86%	7929	52
Kal-CC 2	CC-Oil	90.0	656.3	83%	7455	49	633.4	80%	7424	62
Kal-CC 3	CC-Oil	28.0	74.6	30%	3468	940	70.3	29%	3254	981
Waiau 3	ST-Oil	47.0	53.6	13%	1987	424	44.2	11%	1640	436
Waiau 4	ST-Oil	46.5	60.1	15%	2726	441	48.9	12%	2222	492
Waiau 5	ST-Oil	54.5	90.5	19%	4035	352	75.6	16%	3372	445
Waiau 6	ST-Oil	53.7	74.5	16%	3383	357	60.9	13%	2754	447
Waiau 9	CT-Oil	52.9	41.6	9%	1141	422	39.2	8%	1085	459
Waiau 10	CT-Oil	54.9	83.1	17%	2439	844	79.4	17%	2335	875
CIP-CT	CT-Biodsl	112.2	25.2	3%	519	225	23.8	2%	480	224
AIR-DSG	IC-Biodsl	8.0	3.7	5%	487	197	3.4	5%	454	200
Wind	Wind	123.0	355.6	33%			354.3	33%		
CPV	Solar	149.3	281.9	22%			268.8	21%		
DPV	Solar	400-700	635.1	18%			1111.5	18%		

The production cost simulation results were also analyzed on an hourly basis across the year, an important step when screening for challenging dispatch conditions. This is especially true in scenarios with increasing wind and solar penetration, due to the variable nature of the resources. Some hours of the year will exhibit high wind and solar generation on the grid while others have low or no wind and solar generation.

The uneven dispatch of wind and solar generation across all hours of the year is illustrated in Figure 7. These duration curves sort the wind and solar penetration in total MW delivered and as a percent of system load from highest to lowest throughout the year. From the chart on the right it can be observed that in Scenario 1, some hours of the year approach 50% instantaneous penetration. In Scenario 2, with 300 MW additional DPV, maximum instantaneous penetration approaches 70%, with approximately 1,000 hours at or above 50% instantaneous penetration. Currently EirGrid, the system operator in Ireland, has instituted limits on "simultaneous non-synchronous penetration,"[4] including HVDC imports, to 50% due to stability concerns, with curtailment required afterwards. Other, non-island, regions (such as ERCOT) are experiencing similar levels of instantaneous penetration and are not requiring curtailment, however this threshold is generally viewed as a penetration level that warrants further investigation on grid stability.

[4] SNSP is defined by EirGrid as a measure of non-synchronous generation online as a percentage of total system demand.

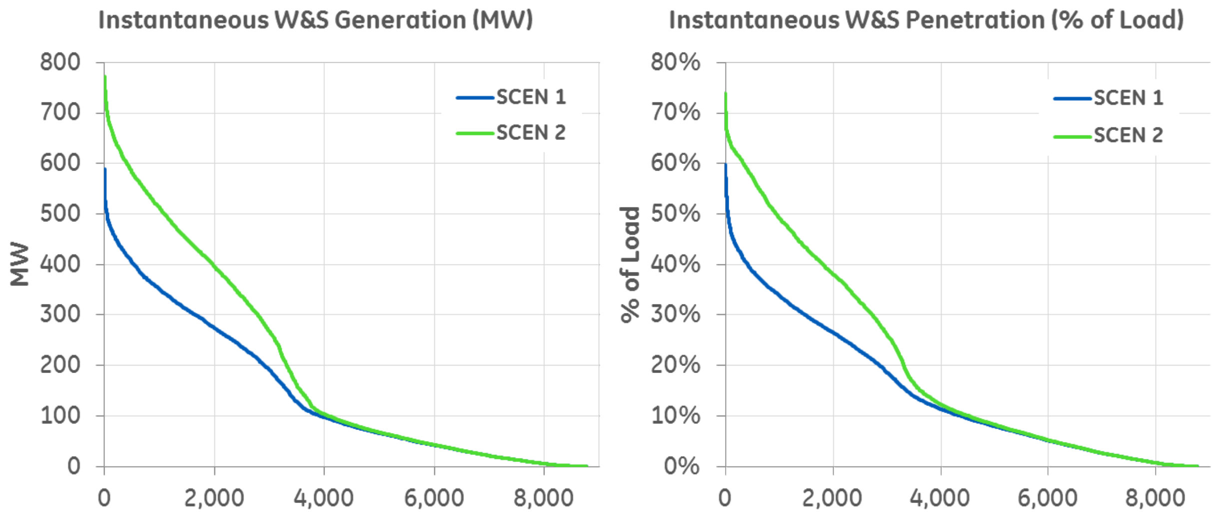

Figure 7: Hourly Duration Curves of Wind and Solar Penetration by Scenario

As discussed previously, increasing levels of DPV on the system affect several factors of system operation that are related to grid frequency performance. Figure 8 shows three of those factors; largest generator contingency, the total thermal commitment (based on MW rating of online generators, not the dispatched output), and the up-reserve provision. The red arrow shows the general direction of the change from Scenario 1 and Scenario 2. The plots show that:

- The largest contingency is the loss of AES at full output for most hours of the year, although AES as somewhat fewer hours at full output in Scenario 2, likely during hours when PV generation is high.
- The thermal unit commitment is slightly lower in Scenario 2 for almost all hours of the year.
- The up-reserve (headroom) of committed thermal generation increases in Scenario 2 during daylight hours because the PV generation causes lower dispatch levels on thermal units.

These three factors, and their impact on frequency response, will be discussed in depth in the following section.

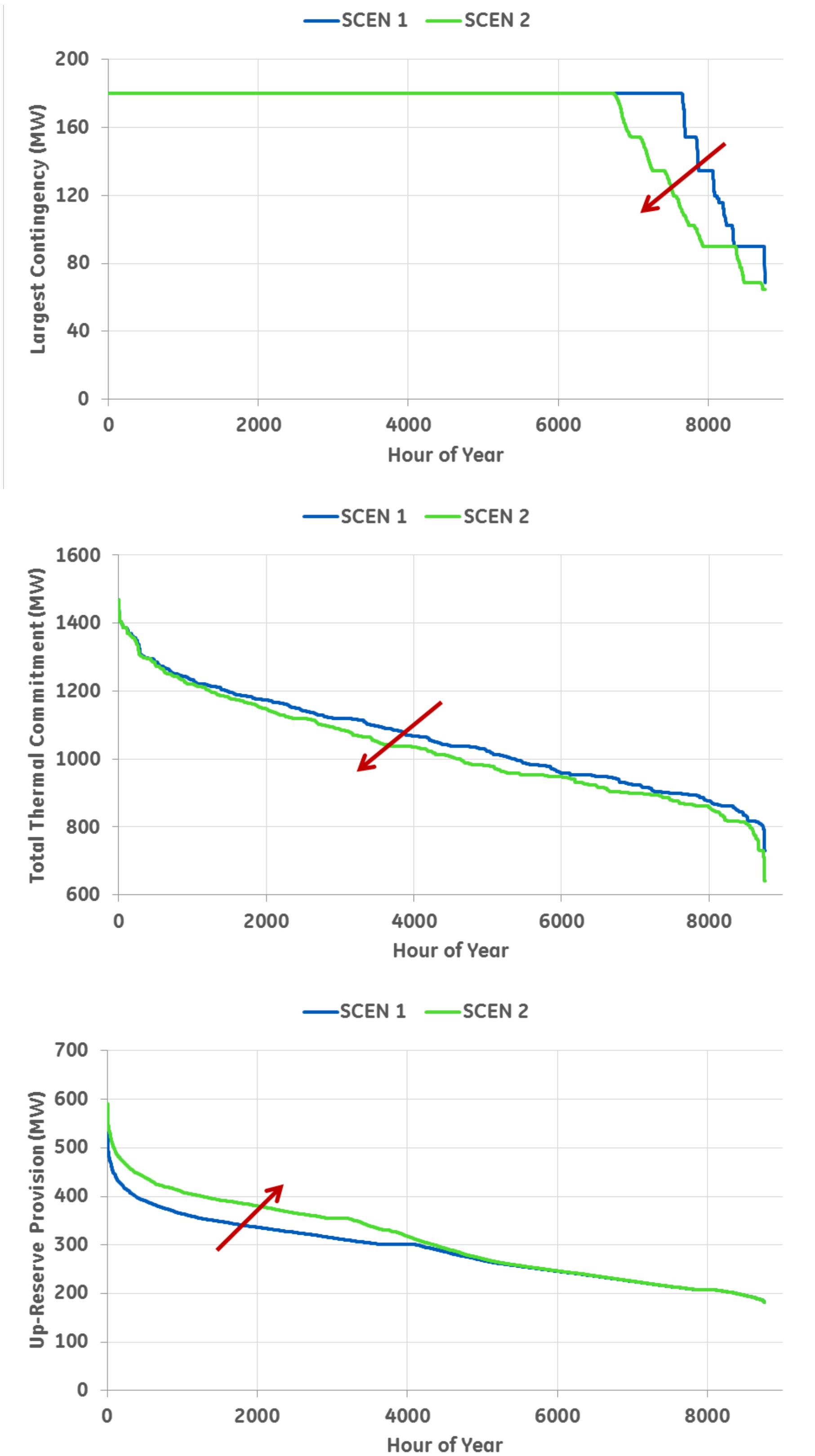

Figure 8: Hourly Duration Curves of Composite Metric Variables by Scenario

3.2 Selecting System Dispatch Conditions

The second step in the analysis included a detailed review of the production cost simulations in an effort to select certain system dispatch conditions to pass from the production cost results to the dynamic frequency response simulations. To do this each hour was quantified based on its expected risk of dynamic stability for a loss of generation event. A new metric was developed that incorporated four important factors to frequency response into a single quantifiable measure. On the Oahu grid, it was assumed that the following four variables would be the largest differentiators in frequency response:

1. **Largest generator contingency:** This variable represents the dispatch (MW) of the largest unit online in a given hour and is used as a measure of the severity of the contingency event. Typically this is the output of AES because it is the largest and most economic unit on the system. However, during a forced outage or maintenance event AES is offline and the largest single contingency may be another unit. During the dynamic simulations, the frequency response of the system will be tested by tripping the largest generator offline and represents the most severe generator contingency event of the hour.
2. **Thermal unit commitment:** This variable was added as a proxy for system inertia and represents the amount of total capacity committed (MW) during every hour. Even if the unit is dispatched at P-min for a given hour, the unit's full rated capacity is counted as being online. The larger the thermal commitment, the more system inertia and overall grid support from conventional generators.
3. **Up-reserves online:** This variable represents the amount (MW) of frequency response available to the system. Also referred to as headroom, it is measured by taking the difference between each unit's maximum net capacity and the corresponding dispatch loading. Only thermal units with frequency response enabled are included in this metric. The more up-reserves online, the more frequency response is available to support the grid during contingency events.
4. **Legacy DPV generation:** This variable represents the MW output of legacy DPV on the system. It is a proxy for the sympathetic DPV tripping that will occur given the inability of legacy DPV inverters (approximately 70 MW of capacity) to ride through frequency disturbances. As a result, with higher legacy DPV output, the system will experience more sympathetic tripping and thus exacerbate the loss of generation contingency event.

In order to combine the four variables listed above into a single metric, a weighting factor (multiplier) was applied to each of the variables based on its expected influence on the magnitude and *direction* of system frequency in response to a generator trip event. Because the metric is meant to define system risk, the sign of the multiplier depends on each variable's likely contribution to a frequency deviation. Therefore, the largest generator contingency and legacy DPV generation variables are multiplied by a positive weighting factor because they are directly related to frequency deviation (the higher the variable the higher the expected frequency deviation). The thermal unit commitment and up-reserves online variables are multiplied by a negative weighting factor because they are inversely related to frequency deviation (the higher the variable the lower the expected frequency deviation).

The magnitude of the weighting factors was also related to the expected impact on system frequency and was developed to strengthen the relationship with the observed frequency response from the dynamic simulations and the calculated metric. A variable that is likely to have a larger relative impact on frequency deviation received a larger weight. The standard deviation of each variable was also taken into account when creating the weighting factors to make the scaling consistent with the overall spread of the sample size selected for dynamic simulations. These weighting factors were adjusted based on the results of the dynamic simulations in Step 3, such that the corresponding quadratic fit of the metric to the simulated frequency nadir was improved and thus provided better estimation of frequency response.

The equation below shows the mathematical formation of the metric.

$$metric = (g_i * w_g) + (c_i * w_c) + (r_i * w_r) + (d_i * w_d)$$

where:

- g is the size of the largest generator contingency.
- c is the amount of committed thermal unit capacity.
- r is the amount of up-reserves online.
- d is the amount of legacy DPV generation.
- i is the observation of each variable for a given hour of the year.
- w is the weighting factor applied to each variable.

The following table provides an example of the metric calculation for two hours of the year in Scenario 1. This calculation shows the difference between a high risk hour (2340) and a lower risk hour (634). The resulting metric in the high risk hour is 0.86 whereas the resulting metric in the lower risk hour is -11. Relative to hour 2340, hour 634 has a lower generator trip contingency, higher thermal unit commitment, higher up-reserves online, and lower DPV generation. As a result the system risk, and thus the metric, is significantly lower. While the number itself does not have any direct meaning, it provides a relative measure for system risk over the course of the year. A higher metric indicates larger expected frequency deviation during a generator trip event, and therefore higher system stability risk in the event of a generator trip.

Table 3: Metric Calculation Example, Hour 2340, Scenario 1

Hour 2340	Largest Contingency (MW)	Thermal Unit Commitment (MW)	Up-Reserves Online (MW)	Legacy DPV Generation (MW)	Summed Metric
Observation	180.0	817.1	320.8	53.7	
Weight	0.0558	-0.0115	-0.0112	0.0713	
Weighted Score	10.05	-9.43	-3.59	3.83	**0.86**

Table 4: Metric Calculation Example, Hour 634, Scenario 1

Hour 634	Largest Contingency (MW)	Thermal Unit Commitment (MW)	Up-Reserves Online (MW)	Legacy DPV Generation (MW)	Summed Metric
Observation	90.0	1172.3	342.3	18.4	
Weight	0.0558	-0.0115	-0.0112	0.0713	
Weighted Score	5.02	-13.53	-3.83	1.31	**-11.0**

The metric calculation shown in the examples above was performed for each hour of the year based on the chronological production cost simulation results from Section 3.1. The resulting metric provides a screening analysis for system risk across each hour of the year. Figure 9 illustrates the average and maximum metric by hour of the day for both scenarios. In general, the metric, and therefore the system risk and expected frequency deviation, is highest during the mid-day (high solar) hours and overnight low-load hours. The early morning and evening hours are least at risk because net load is higher and additional thermal units are online providing conventional ancillary services. With increasing DPV the metric actually decreases during mid-day hour because the additional solar displacement reduces the largest generator contingency and increases the amount of up-reserve provision from the thermal units. The impact on thermal unit commitment is muted because the additional reserve requirement added with the increased DPV requires units to stay online during high wind and solar output periods.

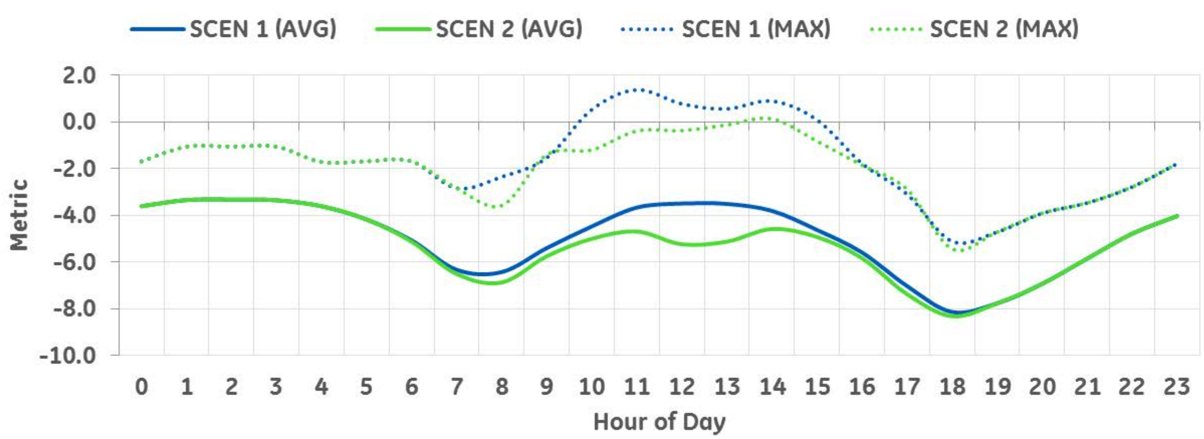

Figure 9: Average and Maximum Metric by Hour of the Day, Scenario 1

Using the 8,760 hourly results from a year of simulation completed in Step 1 (Section 3.1) and the metric calculation discussed above, each hour of the year can be ranked from highest expected risk to lowest based on the system dispatch conditions for a given hour. The resulting duration curve is provided in Figure 10 and created by sorting each hour of the year from highest to lowest based on the calculated metric. From the 8,760 dispatch conditions, a sample of 13 dispatch conditions in each scenario was selected in order to simulate in the dynamic frequency response simulations (Section 3.3) and eventually validate the metric's overall ability to estimate system frequency. The selections were done to include the highest metric hour, a large spread of the overall metric, and to include a spread of the individual variables. The individual hour validation points are highlighted in Figure 10. The dispatch conditions for each validation point, including each generator's power output, overall system load, and legacy DPV generation was passed from the production cost simulations to the dynamic frequency response simulations discussed in the following section.

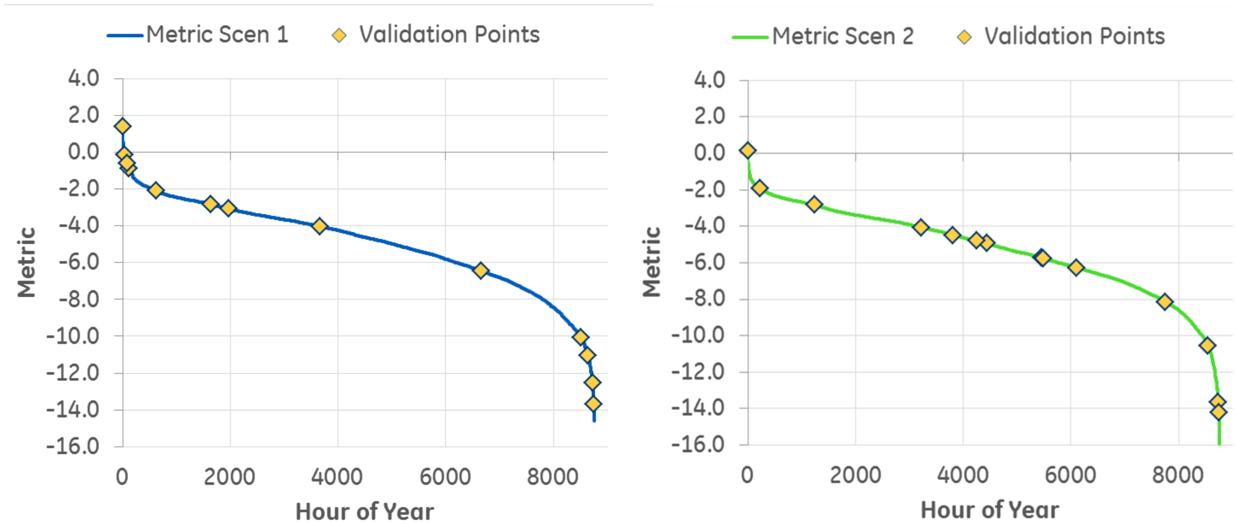

Figure 10: Hourly Metric Duration Curve with Selected Validation Points

3.3 Dynamic Frequency Response Simulations

The dispatch conditions for each selected hour from Step 2 were incorporated into the GE PSLF model for further dynamic simulations. The load, generator output, and distributed PV was setup for each dispatch condition and allocated to individual power flow busses, with full representation of the transmission network model.

In Scenario 1 for example, Hour 2340 (Saturday, April 8th, 11:00 AM) in the production cost simulations was determined to be the most challenging for dynamic frequency response based on the metric calculation. During this hour, the system load was 933 MW (not including house loads at the generators) and DPV output was 306 MW (77% of nameplate capacity). The unit dispatch for that time hour is shown in Figure 11. Note that Kahe 5 and Waiau 8 are offline due to scheduled maintenance or forced outage events. Under this dispatch condition, the loss of AES generation is the single largest contingency on the system (200 MW contingency = 180 MW of net generation + 20 MW of auxiliary loads).

Unit Name	Dispatch (MW)
AES	180.0
Kahe 1	0.0
Kahe 2	0.0
Kahe 3	25.0
Kahe 4	25.0
Kahe 5	0.0
Kahe 6	40.0
Waiau 3	0.0
Waiau 4	0.0
Waiau 5	0.0
Waiau 6	0.0
Waiau 7	25.0
Waiau 8	0.0
Waiau 9	0.0
Waiau 10	0.0
Kalaeloa 1	67.8
Kalaeloa 2	65.0
Kalaeloa 3	0.0
CIP-CT	0.0
AIR-DSG	0.0
H-Power	68.5
Wind	26.2
CPV	105.0
DPV	306.0
System Load	933.4

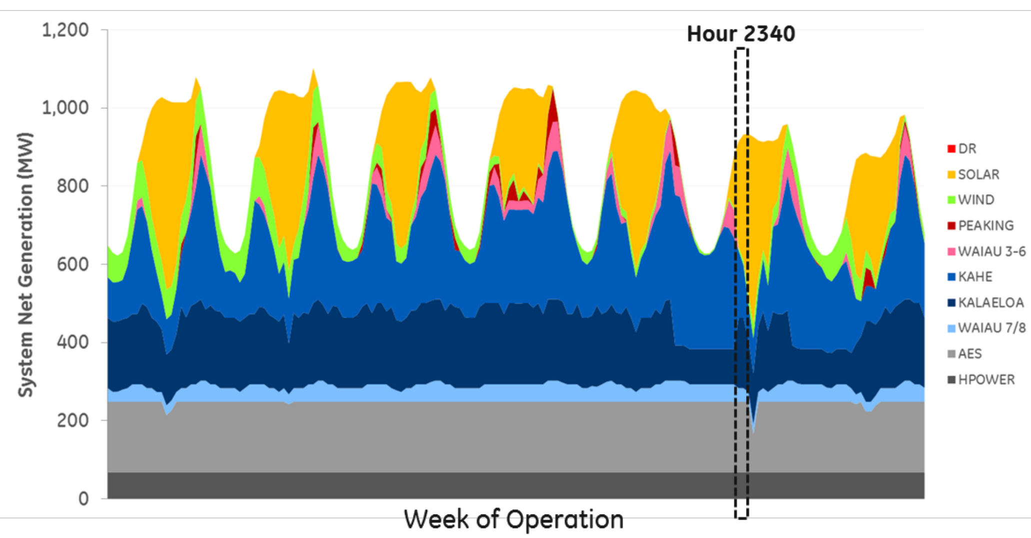

Figure 11: System Dispatch Conditions for Hour 2340, Scenario 1

The results of the dynamic simulation are provided in Figure 12 below. From the figure, the following observations can be made:

- The loss of AES (180 MW), which is triggered at Time = 10 seconds, results in a rapid drop in system frequency.
- During the first second of the event, the legacy PV online (approximately 52 MW) trips offline because it does not have frequency ride-through capability. This exacerbates the event by increasing the loss of generation further (Now 180 MW + 52 MW = 232 MW) and leading to additional decline in system frequency.
- During the frequency decline, the system utilized significant amounts of UFLS, including all of the first 4 blocks (58.9 Hz to 58.1 Hz). The resulting load shed was approximately 220 MW, 24% of system load and interruption of customers. Note also that the effectiveness of the UFLS was decreased by 48 MW of DPV on the load shedding feeders (bottom trace). Although 220 MW of customer load was tripped, the actual reduction was 172 MW net benefit of load shedding for counteracting the frequency decline.
- Eventually the frequency decline arrests at the frequency nadir of 57.8 Hz and begins its backswing and reaching a new stable equilibrium approximately 15 seconds after the generator contingency.
- While UFLS may not be a preferred method of frequency response, it is effective method of last resort, enabling the system to survive this large contingency event and avoid a total system black-out.

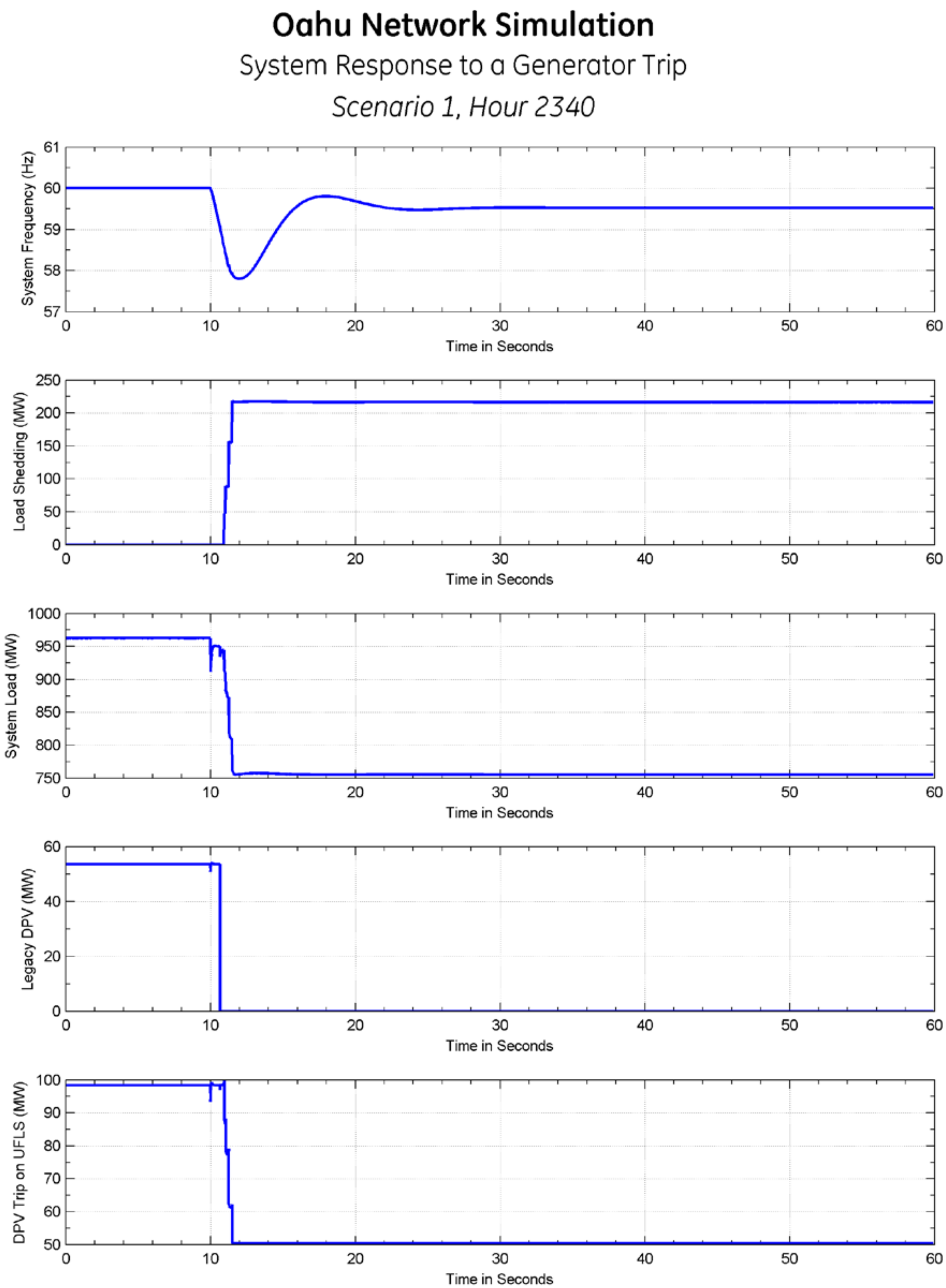

Figure 12: Dynamic Simulation Results, Hour 2340, Scenario 1

The dynamic simulation was also performed on the same hour in Scenario 2. The additional 300 MW of DPV capacity resulted in an additional 229.5 MW of DPV generation online during the hour. Given the same amount of system load, the additional DPV generation displaced generation from other generators on the system and is shown in Table 5. Kahe 4 was cycled offline, Kalaeloa CC-1 generation was reduced by 2.8 MW, and AES generation was reduced by 117 MW to a dispatch of 63 MW (P-Min). This displacement was determined by the production cost simulations and based on system economics. At this point all thermal generators remaining online were must-run units dispatched at P-min. There was still an excess of generation which caused 84.8 MW of curtailed utility-scale solar power. Note that the base case assumption included no frequency response from curtailed utility-scale solar power. This is considered a conservative assumption that will be investigated more in future analysis.

Table 5: System Dispatch Conditions for Hour 2340, Scenario 1 vs Scenario 2

Unit Name	SCEN 1 (MW)	SCEN 2 (MW)	DELTA (MW)
AES	180.0	63.0	-117.0
Kahe 1	0.0	0.0	0.0
Kahe 2	0.0	0.0	0.0
Kahe 3	25.0	25.0	0.0
Kahe 4	25.0	0.0	-25.0
Kahe 5	0.0	0.0	0.0
Kahe 6	40.0	40.0	0.0
Waiau 3	0.0	0.0	0.0
Waiau 4	0.0	0.0	0.0
Waiau 5	0.0	0.0	0.0
Waiau 6	0.0	0.0	0.0
Waiau 7	25.0	25.0	0.0
Waiau 8	0.0	0.0	0.0
Waiau 9	0.0	0.0	0.0
Waiau 10	0.0	0.0	0.0
Kalaeloa 1	67.8	65.0	-2.8
Kalaeloa 2	65.0	65.0	0.0
Kalaeloa 3	0.0	0.0	0.0
CIP-CT	0.0	0.0	0.0
AIR-DSG	0.0	0.0	0.0
H-Power	68.5	68.5	0.0
Wind	26.2	26.2	0.0
CPV	105.0	20.2	-84.8
DPV	306.0	535.5	229.5
System Load	933.4	933.4	0.0

Under these new conditions, the largest generator contingency and severity of the event was reduced by 117 MW, total thermal commitment was reduced by 85 MW (Kahe 4), and the up-reserve provision increased by 57 MW. The frequency response of the system is shown in Figure 13 for the same hour in both Scenario 1 and Scenario 2. Even with the reduced system inertia from Kahe 4 being cycled offline, the net frequency response of the system was improved. The frequency nadir was 58.5 Hz, 0.65 Hz higher than the nadir Scenario 1). Most of this improvement was due to the substantially decreased size of the largest contingency due to the reduced AES generation during the time of the event. As a result, the system frequency deviation was lower and UFLS was reduced from 220 MW to less than 90 MW.

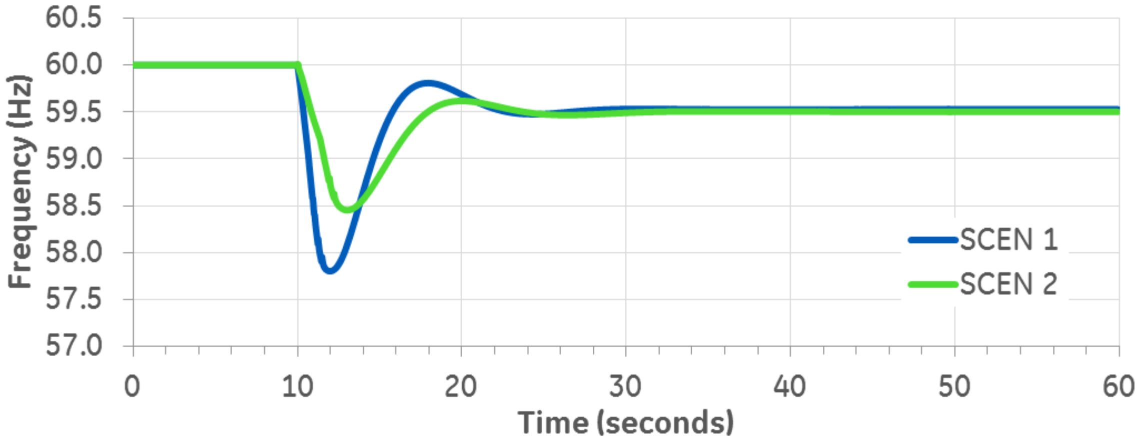

Figure 13: System Frequency Response for Hour 2340, Scenario 1 vs Scenario 2

Note that in this example the system frequency response improved due to the re-dispatch of AES. However, this will not always be the case and there may be times when other thermal units are cycled offline to accommodate the increased DPV generation, but AES is not yet turned back to lower loading levels. As a result, there are hours where system stability will erode with increased DPV generation (as shown in Figure 14). This is caused by reduced UFLS capability, because of the additional DPV generation behind the UFLS breakers being tripped off-line during the contingency event, and fewer thermal units online to respond.

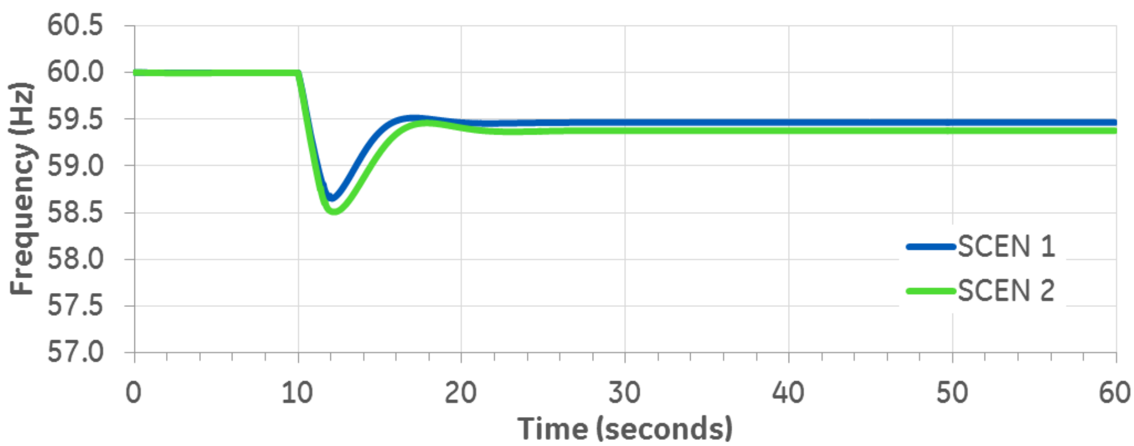

Figure 14: System Frequency Response for Hour 7649, Scenario 1 vs Scenario 2

As a result, under some operating conditions frequency response will improve with increasing DPV and erode in others. Therefore it is important to look at multiple operating points over the course of a year and develop a holistic view of system stability. To ensure this, the dynamic simulations were repeated for each of the 13 dispatch conditions selected in Step 2 (Section3.2) for each scenario. An additional dispatch condition was selected to ensure that the most challenging hour for each scenario (2340 in Scenario 1 and 6087 in Scenario 2) was included in the analysis.

The results of each simulation are provided in the Appendix, with a summary of the frequency nadir, frequency deviation, and UFLS provided in Table 6 for both Scenario 1 and Scenario 2. While the only change in the scenario composition is the amount of DPV capacity on the system, the increased dispatch from the DPV for any given hour may cause secondary changes to the commitment and dispatch of other thermal units on the system. From the table it can be observed that the relationship between the metric and the observed frequency deviation is confirmed between Scenarios 1 and 2. In hours where the metric improves (decreases) from Scenario 1 to Scenario 2 for a given hour, the observed frequency deviation also improves (decreases). In hours where the metric erodes, so does the overall frequency response. The reported UFLS (MW) in Table 6 included only the load and not the DPV generation shed and was rounded to the nearest 10 MW.

Table 6: Observed Frequency Response from Dynamic Simulations

Hour	SCENARIO 1				SCENARIO 2			
	Metric	Nadir (Hz)	Deviation (Hz)	UFLS (MW)	Metric	Nadir (Hz)	Deviation (Hz)	UFLS (MW)
2340	0.9	57.80	2.20	220	-5.0	58.45	1.55	90
1095	-0.6	58.00	2.00	220	-6.3	58.60	1.40	90
3519	-0.9	58.00	2.00	220	-5.5	58.43	1.57	90
1597	-1.2	58.00	2.00	240	-6.3	58.45	1.55	100
5604	-2.3	58.30	1.70	200	-2.5	58.23	1.77	200
1184	-2.8	58.35	1.65	130	-2.8	58.35	1.65	130
8074	-3.1	58.20	1.80	140	-4.1	58.25	1.75	145
2534	-4.6	58.40	1.60	140	-5.4	58.45	1.55	80
7649	-6.5	58.65	1.35	100	-6.3	58.50	1.50	100
4482	-10.1	58.65	1.35	100	-8.1	58.65	1.35	110
634	-11.0	59.30	0.70	0	-10.7	59.13	0.87	0
3091	-12.6	58.95	1.05	0	-13.6	59.05	0.95	0
402	-13.7	59.25	0.75	0	-14.2	59.40	0.60	0
6087					-0.4	58.00	2.00	270

3.4 Estimating Frequency Response

Using the results from the 27 dynamic frequency response simulations (13 in Scenario 1 and 14 in Scenario 2), the final step of the analysis investigated the relationship between the metric developed in Step 2 with the observed frequency response metrics calculated in Step 3. As discussed earlier, the metric was designed to exhibit a direct relationship between the metric and system stability; the higher the metric, the higher the expected frequency deviation and system risk following a generator trip event. Figure 15 shows the relationship of system frequency deviation (dependent variable) as a function of the metric (independent variable) for each of the 27 dynamic simulations conducted in Step 3. This was done for both Scenario 1 (blue markers) and Scenario 2 (green markers) to see the relationship between the frequency nadir and metric with increasing DPV penetration. A quadratic best-fit trend line was then calculated for the 20 operating points as the following equation:

$$y = -0.0005x^2 - 0.1003x + 57.946$$

where x is the composite metric and y is the expected frequency nadir

The resulting function represents the relationship between the metric and the expected frequency nadir. The chart and best-fit line show a clear relationship between the metric developed from the GE MAPS dispatch outputs and the resulting frequency nadir from the PSLF dynamic simulations. In addition, the relationship between the frequency nadir and metric is consistent between Scenario 1 and Scenario 2 observations. While the estimated value is likely not a perfect measure of frequency response, the difference between the estimate and the observation (residual) for the 27 selections is small based on the high R-squared value (a statistical measure of how close the observed data is to the estimated regression line).

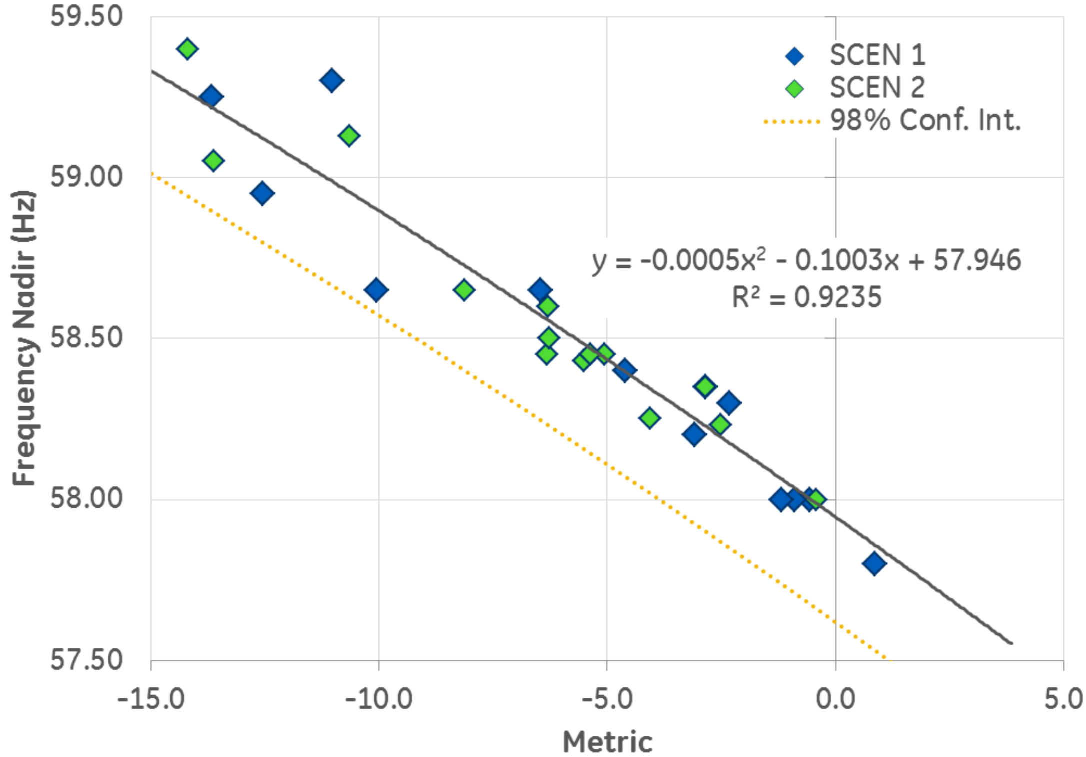

Figure 15: Regression of Frequency Nadir as a Function of the Metric

The quadratic best fit trend line can be used to estimate the frequency nadir, frequency deviation and UFLS for any metric value (and thus system dispatch condition), without the need for additional dynamic frequency response simulations. This was done for all 8,760 hours in both Scenario 1 and Scenario 2. By doing this, the overall system risk can be estimated under each system dispatch condition and ultimately provide a better understanding of trends between scenarios and under different operating conditions. In addition, it allows the reader to draw conclusions about the probability or frequency of different operating conditions, as opposed to previous analysis that only evaluated the most extreme operating points that may only occur rarely throughout the year.

Figure 16 and Figure 17 show the expected magnitude and probability of a frequency deviation for a generator trip event for each hour of the year based on an entire year's worth of system operation. Also demarcated on the charts are lines representing points where the UFLS schemes take place. If the frequency deviation exceeds the threshold for a given block, a breaker will quickly open and reduce over system load in time to reduce the frequency deviation. From these charts it can be seen that while expected frequency deviation to a generator contingency event does not change dramatically, it is reduced when additional distributed PV is added to the system. More importantly, the larger frequency excursions are expected to be reduced, shown by the reduction in the top left portion of the duration curve in Figure 16 and the right hand portion of the histogram. This is an important observation - all other things equal, increased DPV penetration (with frequency ride-through enabled) will not erode grid stability to large N-1 generator trip events under the penetrations evaluated in this study.

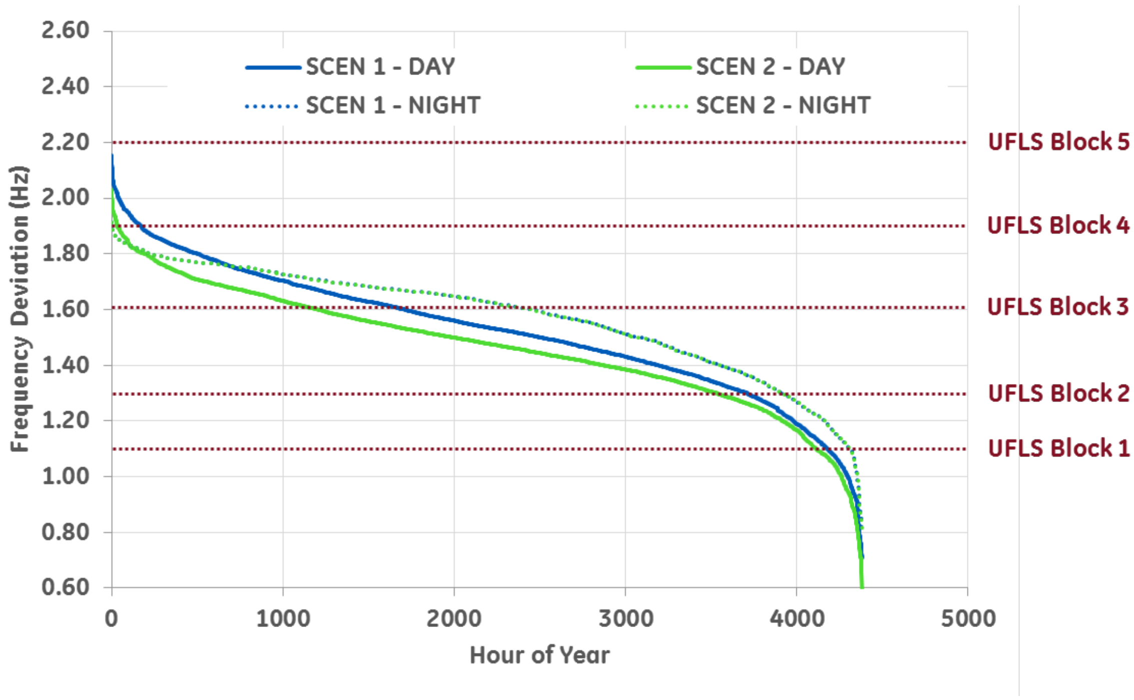

Figure 16: Duration Curve of Expected Frequency Deviation by Scenario

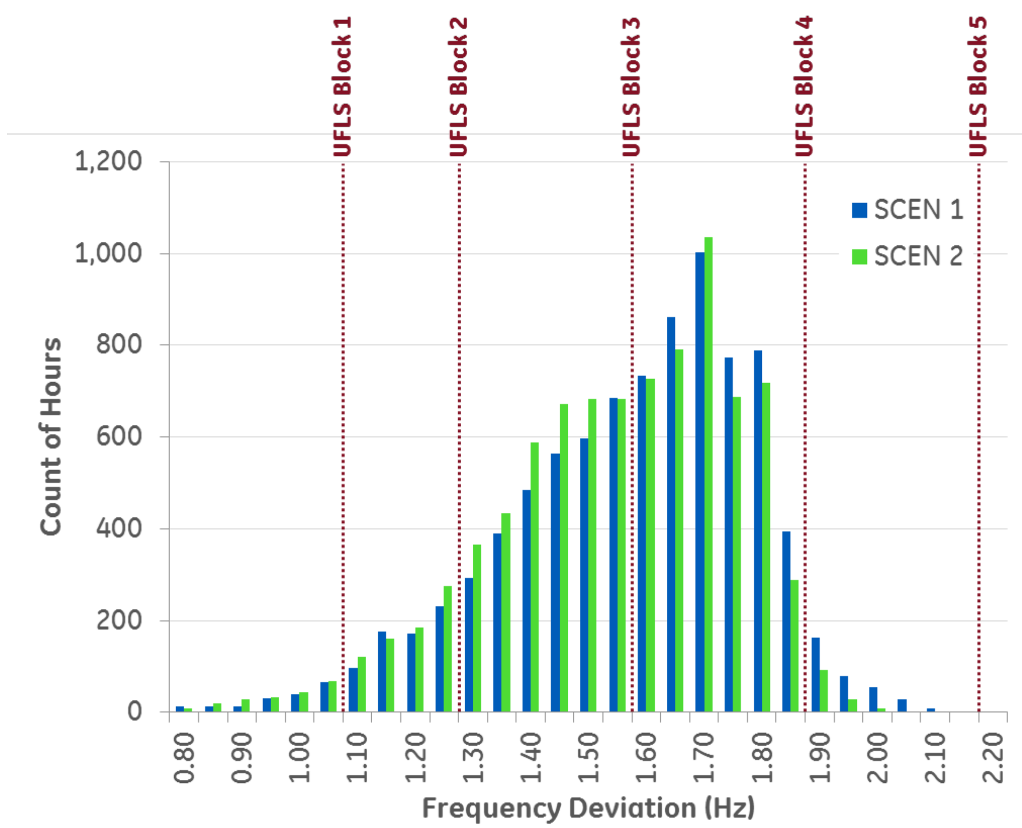

Figure 17: Histogram of Expected Frequency Deviations by Scenario

Given that the expected frequency deviation is calculated for all hours of the year using the quadratic function above, the UFLS can also be estimated for any given hour. In addition, this can be done by taking into account the erosion in the UFLS due to the increased penetration of DPV. As DPV is added to the system the distributed generation reduces the load available behind a distribution feeder. When the feeder is disconnected from the system to shed load, the distributed generation is shed with it. With increasing levels of DPV the capability of the UFLS blocks to arrest system frequency decline are reduced.

Note that in each of the simulations, the UFLS action is on the five blocks, and not on the two kicker blocks, which have long timer delays of 5 and 10 seconds. The kicker blocks are set such that they would not be involved in arresting system frequency decline in the event of a contingency, but instead appear to be intended to bring system frequency closer to its nominal value of 60Hz if, for some reason a large deviation in system frequency persists for a relatively long period of time.

The erosion of UFLS capability is shown in Figure 18. The raw UFLS capability (black dotted line) represents the average load available on the distribution feeders across the different UFLS blocks, in the absence of DPV generation. Scenario 1 (blue) and Scenario 2 (green) lines show the UFLS capability diminishing during mid-day hours. This raises a potential problem; as increased DPV penetration decommits thermal units on the system it will also reduce the net load available to respond (trip offline) during a contingency event.

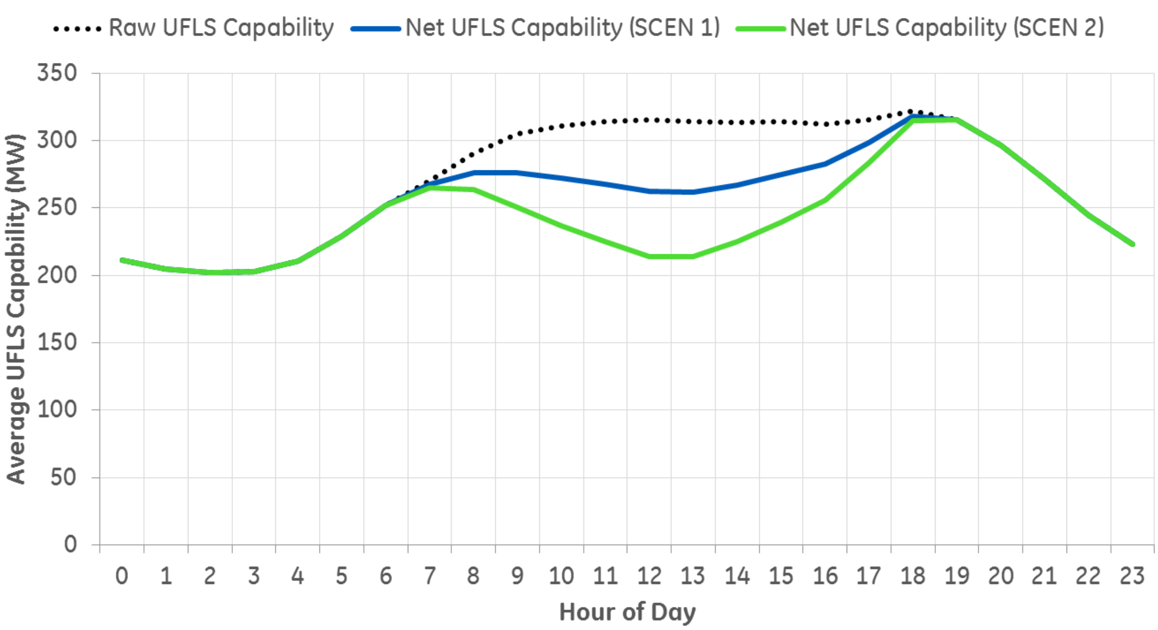

Figure 18: Average UFLS Capability by Hour, Scenario 1 vs Scenario 2

However, the erosion in the UFLS capability is captured in the dynamic simulations, which separated the load and the distributed generation behind the distribution feeders in the UFLS blocks. As a result, only the net load (load minus DPV) was shed from the system in the dynamic simulations. Even with the erosion of UFLS capability the system frequency response is improved (on net over the course of a year) with increased DPV penetration in the scenarios evaluated. This is because while the UFLS provides less response, the contingency events become less extreme (AES backed down to lower loading levels during mid-day hours) and additional thermal units are backed down and can provide additional contingency reserve capability. The improvement in these factors, as shown in the dynamic simulations, outweighs the reduction in UFLS capability. The resulting UFLS, UFGS, and Net UFLS for Scenario 1 and Scenario 2 are provided in Figure 19 for daytime hours. These charts highlight the net improvement in expected UFLS, despite the erosion in capability.

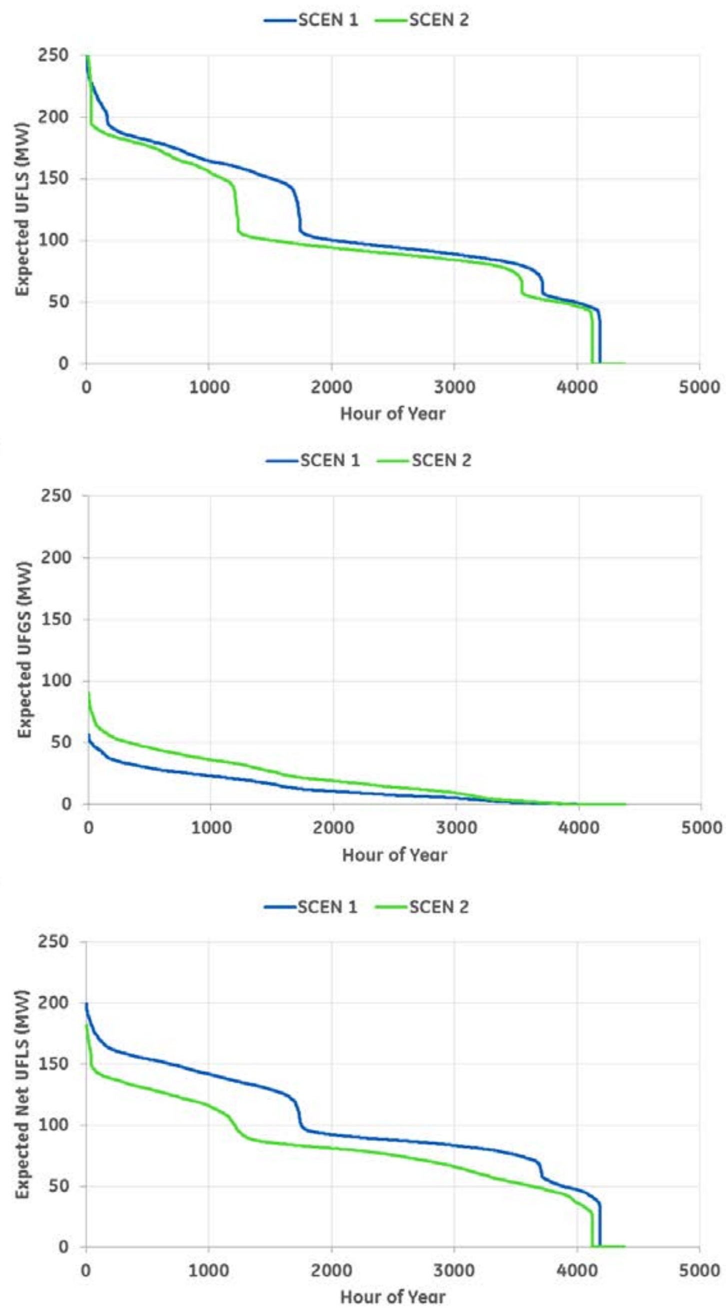

Figure 19: UFLS, UFGS, Net UFLS Duration Curves (Daytime Hours) by Scenario

4 KEY FINDINGS AND RECOMMENDATIONS

4.1 Important Observations

The results of this study provide useful insights to the stable and reliable growth of DPV on the Oahu power grid. However, the following observations should be viewed in the broader context of the study scope and limitations stated previously. In addition, the trends and observations highlighted in this study were based off a system with 700 MW of DPV, 150 MW of CPV and 124 MW of wind. Extrapolating results beyond the renewable penetration studied in this analysis should not be done without further analytical investigation.

- Increased DPV penetration (with frequency ride-through enabled) will not erode grid stability to a generator trip event with the assumptions evaluated in this study.
- Based on the simulations, the grid was able to survive all of the generator contingency events evaluated, even in the most challenging hours of operation
- While the expected frequency response in some hours may have been reduced when adding 300 MW of DPV, the net result when evaluating the entire year of operations is a slight improvement in system frequency response to a generator contingency.
- With increasing DPV the system frequency response to a generator contingency event improves during peak solar, mid-day hours because the additional solar displacement reduces the largest generator contingency and increases the amount of up-reserve provision from the thermal units.
- The increased penetration of DPV is decreasing the net load available to respond during UFLS events. This erosion could have a significant impact on the efficacy of UFLS. In addition, if the grid operator does not have real-time knowledge of the levels of DPV generator on particular feeders, an UFLS event could actually trip off additional generation (negative net load) if DPV penetration gets high enough.
- Although annual energy served by wind and solar generation is below 22% in the scenarios evaluated, there are times when instantaneous penetration approaches 70%, with approximately 1,000 hours at or above 50% instantaneous penetration.
- While increased DPV penetration analyzed in this study increased the overall up-reserve provision available to the system, the down-reserve provision was decreased substantially. This will have important implications to load rejection contingency events and needs to be evaluated closely in the next stage of this study.
- The turndown of AES and other large generators to lower loading levels during high solar output is a primary driver of the reduced system risk. It should be noted that this is an alignment of economic and stability objectives. However, if AES remains dispatched at full output then the severity of the contingency event is not reduced. IN these circumstances curtailed wind and solar can provide the additional frequency response required to compensate for the larger contingency event.

4.2 Future Research

While the analysis outlined throughout this report provides valuable insight to grid stability concerns on Oahu with increasing DPV, other questions critical to assessing grid stability remain. It is therefore suggested that the following items be evaluated in future study work, as the islands strive forward towards meeting the RPS goals. Much of this material will be covered in future stages of this study using a similar modeling approach and project team.

- **Load Trips:** A similar analysis to the one in this report needs to be conducted on load trip contingency events. As thermal units are backed down to lower loading levels, it will be important to evaluate over-frequency response in detail and to what degree both utility-scale and distributed renewables and provide frequency response.
- **Short Circuit Ratios:** As the penetration of grid-connected power electronic equipment like wind, central & distributed PV, and storage increases, the electrical "stiffness" of the grid tends to decrease, which could lead to voltage and control instabilities on the grid. Because the risk of instability is highly dependent on the electrical stiffness of the grid, which can change suddenly and many times a day, the instantaneous renewable penetration is often used as a proxy for this risk. This analysis will quantify the strength of the Oahu grid under various expected operating conditions to help assess the risk of power electronic equipment instability.
- **Higher Renewable Penetration:** While this study evaluated a doubling of solar capacity on Oahu, wind and solar penetration remained below 25% and well below future RPS targets. Scenarios with higher renewable penetration must be evaluated to determine frequency response at higher penetration.
- **Evaluate Different Systems:** The quadratic equation formulated in this study proved to be a good predictor of frequency response. However it is unique to the current Oahu grid configuration. As the thermal resource mix on Oahu changes or this analysis is brought to additional power systems, the metric needs to be recalibrated based on additional dynamic simulations.
- **Grid Support from Wind & Solar:** While not evaluated in this study, curtailed utility-scale wind and solar can provide significant benefits for frequency response. While curtailing wind and solar specifically to provide this ancillary service may not be economic, utilizing already curtailed generation due to other constraints will increase grid support.
- **Examine Mitigations:** Although grid stability was not shown to deteriorate with increasing DPV penetration in this study, several mitigations should be evaluated to improve frequency response, reduce UFLS, and increase grid stability, including:
  - Demand Response
  - Energy Storage & Electric Vehicles
  - Legacy Inverter Retrofits
  - Dynamic UFLS Schemes
  - Minimum Number of Units Online
  - Spinning Reserve Adjustments
  - AES Re-dispatch